Highly flexible polymeric optical waveguide for out-of-plane optical interconnects

Xinyuan Dou[1], Xiaolong Wang[2], Xiaohui Lin[1], Duo Ding[1], David Z. Pan[1] and Ray T. Chen[1*], *IEEE Fellow*

[1]Department of Electrical and Computer Engineering, the University of Texas at Austin, Austin, TX, 78758, USA
[2]Omega Optics, Inc. Austin, TX 78759 USA
**chen@ece.utexas.edu*

Abstract: In this paper, we reported high speed optical test on polymeric optical waveguide array with embedded 45° micro-mirrors on flexible substrate for out-of-plane optical interconnects. The waveguide array was bent with curvature ranging from 61mm to 5mm. As the bending radius decreases, the average insertion loss increases from 3.4dB to 7.7dB for single-mode fiber (SMF) coupling and from 5.5dB to 7.9dB for multi-mode fiber (MMF) coupling, respectively. Eye-diagrams under such bending conditions show that the Q factor decreases from 8.0 to 6.1 and the calculated bit error rate (BER) increases from 10^{-16} to 10^{-10} at 10Gbps.

OCIS codes: (200.4650) Optical interconnects; (130.5460) Polymer waveguides; (230.0230) Optical devices.

References and Links

1. O. Ishida, and T. Wang, "100 gigabit Ethernet transport," IEEE Commun. Mag. 48, S4 - S4, (2010).
2. R. T. Chen, L. Lin, C. Choi, Y. Liu, B. Bihari, L. Wu, S. Tang, R. Wickman, B. Picor, M. K. Hibbs-Brenner, J. Bristow, and Y. S. Liu, "Fully Embedded Board level Guided-wave Optoelctronic Interconnects," Proc. IEEE, 88, 780-793 (2000).
3. F. E. Doany, C. L. Schow, C. W. Baks, D. M. Kuchta, P. Pepeljugoski, L. Schares, R. Budd, F. Libsch, R. Dangel, F. Horst, B. J. Offrein, and J. A. Kash, "160 Gb/s Bidirectional Polymer-Waveguide Board-Level Optical Interconnects Using CMOS-Based Transceivers," Advanced Packaging, IEEE Transactions on, 32(2),345-359 (2009).
4. X. Y. Dou, X. L Wang, H. Y. Huang, X. H. Lin, D. Ding, D. Z. Pan, and R. T. Chen, "Polymeric waveguides with embedded micro-mirrors formed by Metallic Hard Mold," Opt. Express 18, 378-385 (2010).
5. L. Wang, X. Wang, W. Jiang, J. Choi, H. Bi, and R. T. Chen, "45° polymer-based total internal reflection coupling mirrors for fully embedded intraboard guided wave optical interconnects," Appl. Phys. Lett. 87(14), 141110 (2005).
6. X. Wang, W. Jiang, L. Wang, H. Bi, and R. T. Chen, "Fully Embedded Board-Level Optical Interconnects From Waveguide Fabrication to Device Integration," J. Lightwave Technol. 26(2), 243-250 (2008).
7. M. Hikita, R. Yoshimura, M. Usui, S. Tomaru, and S. Imamura, "Polymeric optical waveguides for optical interconnections," Thin Solid Films, 331(1), 303-308 (1998).
8. F. Wang, F. Liu, and A. Adibi, "45 Degree Polymer Micromirror Integration for Board-Level Three-Dimensional Optical Interconnects," Opt. Express, 17(13), 10514-10521 (2009).
9. W. J. Lee, S. H. Hwang, J. W. Lim, and B. S. Rho, "Polymeric Waveguide Film With Embedded Mirror for Multilayer Optical Circuits," IEEE Photon. Technol. Lett. 21(1), 12-14 (2009).
10. J. Van Erps, N.Hendrickx, C. Debaes, P. Van Daele, and H. Thienpont, "Discrete Out-of-Plane Coupling Components for Printed Circuit Board-Level Optical Interconnections" IEEE Photon. Technol. Lett. 19(21), 1753-1755 (2007).
11. N. Hendrickx, J. Van Erps, E. Bosman, C. Debaes, H. Thienpont, and P. Van Daele, "Embedded Micromirror Inserts for Optical Printed Circuit Boards," IEEE Photon. Technol. Lett. 20(20), 1727-1729 (2008).
12. B. S. Rho, W. J. Lee, J. W. Lim, G. W. Kim, C. H. Cho, and S. H. Hwang, "High-reliability flexible optical printed circuit board for opto-electric interconnections," Opt. Eng. 48(1), 015401 (2009).
13. B. Howley, X. L. Wang, Y. H. Chen, and Ray T. Chen, "Experimental evaluation of curved polymer waveguides with air trenches and offsets," J. Appl. Phys. 100, 023114 (2006).

#128759 - $15.00 USD Received 20 May 2010; revised 7 Jul 2010; accepted 8 Jul 2010; published 16 Jul 2010

1. Introduction

The demand for increasing bandwidth, driven by high-definition video sharing, network communications and many other applications, draws significant research efforts devoted to the development of high speed data communication for carrier networks and enterprise applications [1]. Challenges on electrical copper interconnects at high frequency make optical interconnect technologies become a promising alternative to conventional electrical interconnects at different levels, such as rack-to-rack, board-to-board and board level chip-to-chip interconnects [2-11]. Recent reported board level optical interconnects between two optomodules achieved an aggregated 160 Gb/s bidirectional data rate through 32 polymer waveguides operating at 10Gb/s [3]. Highly flexible polymeric waveguide for optical interconnects also has advantages in the application of next generation technology mobile devices, such as personal laptops, digital cameras and foldable mobile phones [12]. These foldable mobile devices require not only high speed, error free data transmission, but also the highly flexible interconnect near the hinge area, where the waveguide faces out-of-plane bending frequently. The performance of polymeric waveguide under out-of-plane bending needs to be investigated in order to meet the high requirement of future mobile devices, such as smaller hinge structure and higher data transmission speed.

We recently reported fabrication of optical waveguide array with embedded 45° micro-mirrors on flexible substrate using metallic Ni hard mold [4]. In this paper, we investigated the out-of-plane bending effect on the waveguide array performance at different bending radius. The insertion losses of 12-channel waveguide array were measured using single-mode fiber(SMF) or multimode fiber(MMF) as the input. High speed optical test at 10Gbps was also carried out on the waveguide under out-of-plane bending conditions. By studying the insertion loss and high speed tests, the critical bending condition was found and beyond that the device performance will be degraded significantly. This is useful in the future application in terms of avoiding performance degradation caused by the out-of-plane bending effect.

2. Insertion loss measurement on the bended waveguide

Polymeric waveguide array device was achieved by UV imprint method using the electroplated Ni mold. The fabrication details were described in reference [4]. The waveguide cladding and core materials are WIR30-450 and WIR30-470, respectively, purchased from ChemOptics Inc. The corresponding refractive indices of the waveguide cladding and core are 1.45 and 1.47 at 850nm, respectively. The flexible TOPAS substrate is TEONEX film from Dupont Teijin Films Inc. The fabricated waveguide has a 50μm×50μm core, 15μm thick top and bottom claddings and 4.8cm length. One of the advantages of our waveguide array is that the whole device can be bent out-of-plane due to its flexible substrate. The performance degradation caused by the bending is needed to be studied. Here we carried out a series of insertion loss measurements on the bended waveguide at different bending radii at 850nm wavelength. Fig.1 shows schematic setup for the bending test. The device was fixed onto the curved surface with the bending radii of 61.1mm, 30.6mm, 20.4mm, 15.3mm, 12.2mm, 10.2mm, 9.2mm, 7.6mm and 5.0mm, respectively. The corresponding bending angles are 45°, 90° and 135° for 61.1mm, 30.6mm and 20.4mm, respectively, limited by the waveguide length. The bending angles for the radii at 15.3mm or less are all 180°. The performance without any bending was also measured for comparison. A 1 meter long 9/125μm single-mode fiber (SMF) and a 50/125μm multi-mode fiber (MMF) were used to couple the light into the waveguide. A photodetector was placed at the output end to measure the output light intensity.

#128759 - $15.00 USD Received 20 May 2010; revised 7 Jul 2010; accepted 8 Jul 2010; published 16 Jul 2010

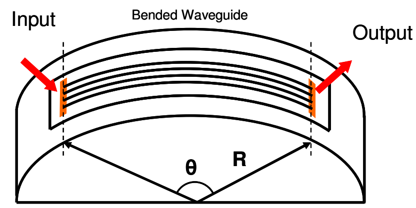

Fig. 1. Schematic view of the bended waveguide array on a semi-column surface

The insertion loss measurement results of the waveguide array at flat condition and at selected bending radii of 61.1mm, 20.4mm, 10.2mm, 9.0mm and 5.0mm were shown in Fig.2a-f. In these figures, red and green bars correspond to the losses measured by SMF and MMF, respectively. SMF has much smaller core diameter and higher coupling efficiency than MMF. So that the loss measured by SMF is smaller than that measured by MMF. From these figures we see that as the bending radius decreases from flat condition to 5.0mm, the insertion loss increases due to the bending effect of the whole device. In order to wipe off the random errors in the measurement and find out the bending effect, we calculated the average insertion loss of 12 channels at each bending radius. Fig.3a gives the calculation results for all 9 different bending radii. The points on the most right hand side correspond to flat condition. From flat condition to 5mm bending radius, the average insertion loss increases from 3.4dB to 7.7dB and 5.5dB to 7.9dB for SMF and MMF, respectively. The total degradations caused by bending are around 4.3dB and 2.4dB for SMF and MMF, respectively. From Fig. 3a we can see the insertion loss increases significantly only when the bending radius is below 9.0mm. The measured bending loss is a little higher than the simulation results of similar curved waveguide [13]. The other phenomena is that as the bending radius decreases, the average insertion loss difference measured between SMF and MMF decreases from 2.0dB to 0.2dB(Fig.3b). We believe that as the bending radius decreases, the loss due to bending becomes dominant over the coupling loss or propagation loss, and it's independent on SMF or MMF.

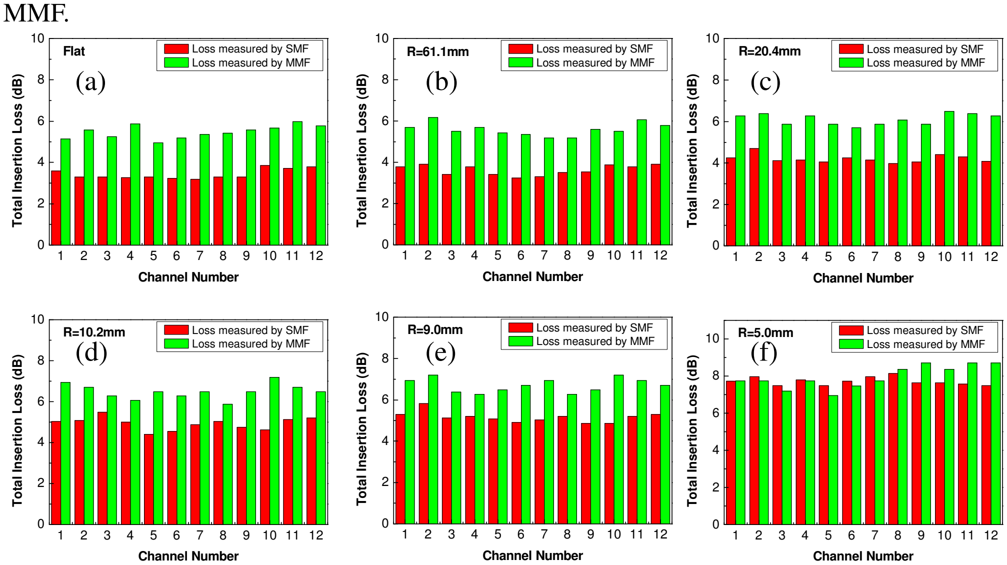

Fig. 2. Insertion loss measurements for 12 channels at different bending radius (a)flat condition, (b)61.1mm, (c)20.4mm, (d)10.2mm, (e)9.2mm and (f)5.0mm. Red and green bars are for SMF and MMF coupling, respectively.

#128759 - $15.00 USD Received 20 May 2010; revised 7 Jul 2010; accepted 8 Jul 2010; published 16 Jul 2010

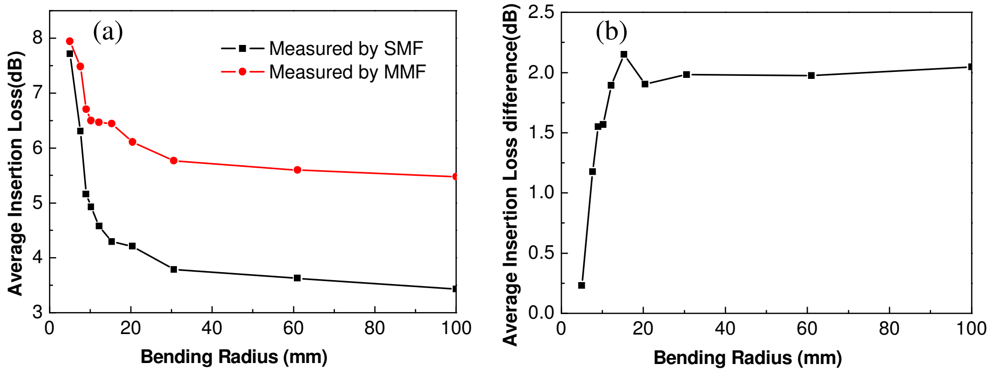

Fig. 3. Bending radius dependence of (a) average insertion loss measured by SMF coupling (black) and MMF coupling (red) (b) average insertion loss difference measured between SMF and MMF.

3. High speed optical test on the waveguide under bending

In order to study the high speed performance degradation of the waveguide array under bending, optical test at 850nm was carried out on the fabricated device. VCSELs and photodiodes (PD) operating at 850nm were purchased from Finisar Co., which meet the performance requirements for 10Gbps data communication over multimode optical fibers. The optical assembly was designed to interface either 50μm or 62.5μm multimode fiber. The schematic setup (Fig. 4a) and actual setup (Fig. 4b) of the high speed optical test are shown. The differential pulse signal and the DC bias were connected to an evaluation board by two high frequency bias tees, on which the 10Gbps VCSEL was mounted, shown in Fig.4c. The combined bias was used to drive the VCSEL to emit modulated light intensity. A multi-meter was connected to monitor the driven current for the VCSELs. The modulated optical signal from VCSEL was coupled into the waveguide by 45° TIR micro-mirrors through a 50/125μm multimode fiber. After propagation through the waveguide, the light was coupled out by the surface-normal 45° TIR micro-mirrors into the 62.5/125 μm multimode fiber. Typical DC bias for the VCSEL is about 1.90V with a current 5.8mA, which produces an emitting power of 920μW at 850nm. The random signal level is ±0.3V. The other end of MMF was connected to the high speed photodiode operating at 850nm, which was mounted on another evaluation board, as shown in Fig.4d. The signal response from the photodiode was connected to the oscilloscope for the eye diagram observation. DC bias applied to the photodiode for efficient converting is 3.3V. The modulation speed of the VCSEL signal can be controlled by signal generator through PC software, which has a range from 1Gps to 10Gps.

#128759 - $15.00 USD Received 20 May 2010; revised 7 Jul 2010; accepted 8 Jul 2010; published 16 Jul 2010

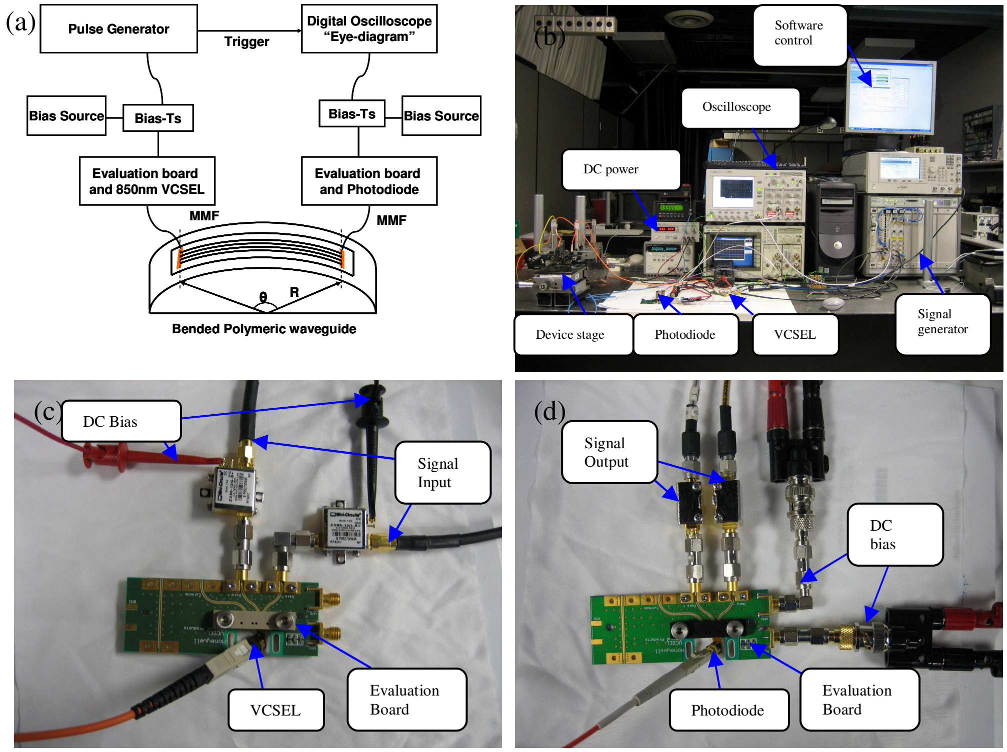

Fig. 4. (a) Schematic and (b) actual view of the high speed test setup for the bended waveguide. (c) VCSEL mounted on an evaluation board, with DC bias and signal input connections. (d) Photodiode mounted on an evaluation board, with DC bias and signal output connections.

At flat condition or 0° bending angle condition, we measured the eye-diagrams with frequencies from 1Gbps to 10Gbps. All eye-diagrams are widely open from 1Gbps to 10Gbps. The eye-diagrams at different bending curvatures were also successfully obtained. Fig.5a-f show the selected eye-diagrams as bending radius decreases from flat condition to 5.0mm. The signal-to-noise ratio or Q factor was also measured at each bending radius. After achieving the Q factors, we calculated the bit error rate (BER). The relation between the Q-factor and BER is given by: $BER = (1/2)\times erfc(Q/\sqrt{2})$ [6], if assuming the presence of Gaussian distributed noises.

#128759 - $15.00 USD Received 20 May 2010; revised 7 Jul 2010; accepted 8 Jul 2010; published 16 Jul 2010

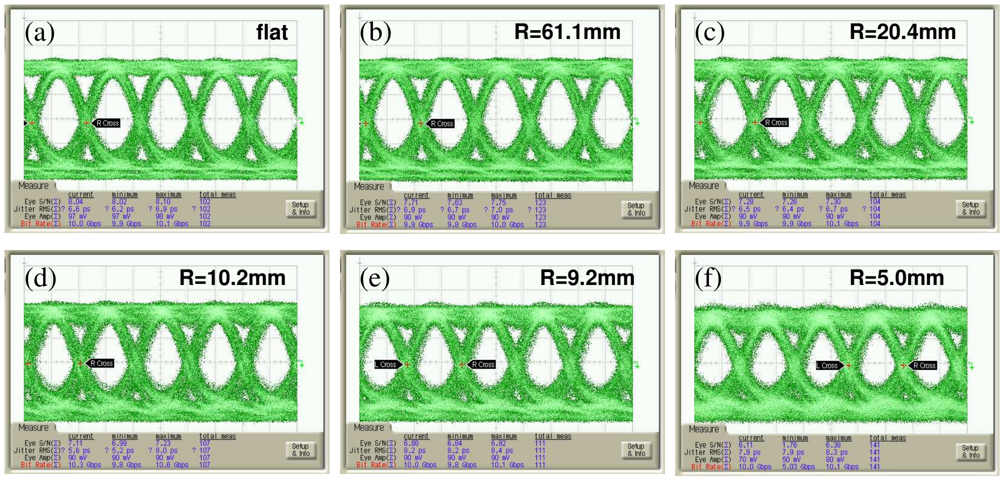

Fig. 5. Selected eye-diagrams at 10Gbps with bending radii at (a)flat condition, (b)61.1mm, (c)20.4mm, (d)10.2mm and (e)9.2mm, (f)5.0mm

The frequency dependence of Q factors and calculated bit error rate (BER) from 1Gbps to 10Gbps at 0° bending condition are shown in Fig.6a. As the bit rate increases from 1Gbps to 10Gbps, the Q factor decreases from 14.4 to 8.0. Q factors at 7Gbps and 8Gpbs increase slightly due to the photodiode response properties. The calculated BER increases from around 10^{-45} at 1Gbps to 10^{-16} at 10Gbps. Fig.6b shows the bending radius dependence of Q factor and calculated BER at 10Gbps. From flat condition to 5mm bending radius, the Q factor decreases from 8.0 to 6.1 and the BER increases from 10^{-16} to around 10^{-10}. The degradations of Q factor and BER are expected due to the increasing insertion loss of the bending waveguide. From the calculation, in order to maintain BER less than 10^{-12}, the bending radius should be above 9.0mm. This is consistent with our insertion loss measurement results under bending conditions. From the application point of view, 9.0mm bending radius is small enough for some large devices, such as some personal laptops, computers. For some smaller devices, such as personal mobile phones, further research work is needed to reduce the critical bending radius to be less than 5.0mm with 10^{-12} or less BER at 10Gbps, such as using lower propagation loss, higher core and cladding index contrast polymer materials, more flexible substrate, higher efficient coupling techniques and optimizing the fabrication process.

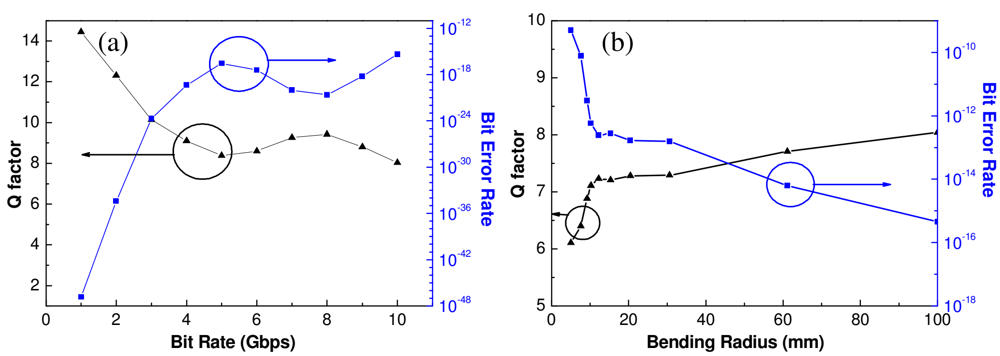

Fig. 6. Q factor and Bit Error Rate(BER) dependence on (a) the bit rate without bending and (b) the bending radius

4. Summary

In this paper, we have successfully measured the bending effect on the insertion losses and the high speed performance of the waveguide array which was fabricated by UV imprint method

#128759 - $15.00 USD Received 20 May 2010; revised 7 Jul 2010; accepted 8 Jul 2010; published 16 Jul 2010

using metallic hard mold. As bending radius decreases, the average insertion loss at 850nm of the 12 channels increases both for SMF and MMF. Eye diagrams with 10Gbps random signals at different bending radius were also successfully achieved. The signal-to-noise ratios, Q factors, were obtained at each bending condition. The bit-error-rate (BER) was calculated by assuming the presence of Gaussian distributed noises at each frequency.

Acknowledgements

This work is supported by the National Science Foundation. The fabrication and characterization facilities at UT MRC are supported through NNIN program.

#128759 - $15.00 USD Received 20 May 2010; revised 7 Jul 2010; accepted 8 Jul 2010; published 16 Jul 2010